Published in final edited form as:
*Chem Res Toxicol*. 2011 August 15; 24(8): 1297–1303. doi:10.1021/tx200188j.

# Identification and Quantification of DNA Adducts in the Oral Tissues of Mice Treated with the Environmental Carcinogen Dibenzo[*a,l*]pyrene by HPLC-MS/MS

**Shang-Min Zhang**[†,#], **Kun-Ming Chen**[†,#], **Cesar Aliaga**[†], **Yuan-Wan Sun**[†], **Jyh-Ming Lin**[†], **Arun K. Sharma**[‡], **Shantu Amin**[‡], and **Karam El-Bayoumy**[*,†]

[†]Dept. of Biochemistry and Molecular Biology, Penn State College of Medicine, Hershey, PA 17033

[‡]Dept. of Pharmacology, Penn State College of Medicine, Hershey, PA, 17033

## Abstract

Tobacco smoking is one of the leading causes for oral cancer. Dibenzo[*a,l*]pyrene (DB[*a,l*]P), an environmental pollutant and a tobacco smoke constituent, is the most carcinogenic polycyclic aromatic hydrocarbon (PAH) tested to date in several animal models (target organs: skin, lung, ovary and mammary tissues). We have recently demonstrated that DB[*a,l*]P is also capable of inducing oral cancer in mice; however its metabolic activation to the ultimate genotoxic metabolite dibenzo[*a,l*]pyrene-11,12-dihydrodiol-13,14-epoxide (DB[*a,l*]PDE) in mouse oral cavity has not been examined. Here we developed a liquid chromatography-tandem mass spectrometry (LC-MS/MS) method to detect and quantify (±)-*anti*-DB[*a,l*]PDE-dA adducts in oral tissues of mice treated with DB[*a,l*]P. [$^{15}N_5$]-(±)-*anti*-DB[*a,l*]PDE-$N^6$-dA adducts were synthesized as internal standards. The stereoisomeric adducts were characterized by MS, NMR and CD analysis. The detection limit of the method is 8 fmol with 100 μg digested DNA as the matrix. Two adducts were detected and identified as (−)-*anti-cis* and (−)-*anti-trans*-DB[*a,l*]PDE-dA in the oral tissues of mice following direct application of DB[*a,l*]P (240 nmol per day, for 2 days) into the oral cavity, indicating that DB[*a,l*]P is predominantly metabolized into (−)-*anti*-DB[*a,l*]PDE in this target organ. We also compared the formation and removal of adducts as a function of time, following direct application of DB[*a,l*]P (24 nmol, 3 times per week for 5 weeks) into the oral cavity of mice. Adducts were quantified at 48 h, 1, 2 and 4 weeks after the last dose. Maximal levels of adducts occurred at 48 h, followed by a gradual decrease. The levels (fmol/μg DNA) of (−)-*anti-trans* adducts (4.03±0.27 to 1.77±0.25) are significantly higher than (−)-*anti-cis*-DB[*a,l*]PDE-dA adduct (1.63±0.42 to 0.72±0.04) at each time point ($p < 0.005$). The results presented here indicate that the formation and persistence of (−)-*anti*-DB[*a,l*]PDE-dA adducts may, in part, contribute to the initiation of DB[*a,l*]P-induced oral carcinogenesis.

## INTRODUCTION

Head and neck cancer is the fifth most common cancer worldwide, with oral cancer being the most common form (1). Tobacco smoking is causally associated with cancer of the oral cavity (including lip and tongue) (2;3). Based on animal studies, polycyclic aromatic

[*]**CORESPONDING AUTHOR FOOTNOTE** To whom correspondence should be addressed. Department of Biochemistry and Molecular Biology, Pennsylvania State College of Medicine, Hershey, PA 17033. Tel: 717-531-1005. Fax: 717-531-0002. kee2@psu.edu.
[#]The authors have contributed equally to this manuscript.

**SUPPORTING INFORMATION:**
This material is available free of charge via the Internet at http://pubs.acs.org.

hydrocarbon (PAH) and tobacco specific nitrosamines are the most likely causes of oral cancer in smokers (4). The PAH dibenzo[*a,l*]pyrene (DB[*a,l*]P), also known as dibenzo[*def,p*]chrysene, is an environmental pollutant and a tobacco smoke constituent (5–8). DB[*a,l*]P was identified in cigarette smoke but not quantified (9). DB[*a,l*]P is the most potent carcinogenic PAH tested so far in several animal studies, including mouse skin, lung and ovary, as well as rat mammary gland (7). We have recently showed that DB[*a,l*]P was also capable of inducing oral cancer in mice (10). However, the metabolic activation of DB[*a,l*]P and its genotoxic effect in mouse oral cavity have not previously been examined. It is generally accepted that PAHs exert their mutagenic effects and initiate the carcinogenic process through the generation of metabolites that lead to the formation of potentially mutagenic covalent DNA adducts which can cause miscoding and mutations (11). As a procarcinogen, the genotoxic potency of DB[*a,l*]P requires enzymatic activation predominantly by the cytochrome P450 1A1, 1B1 (CYP1A1 and 1B1) and microsomal epoxide hydrolase (EPHX1) to yield the ultimate carcinogenic metabolite dibenzo[*a,l*]pyrene-11,12-dihydrodiol-13,14-epoxide (DB[*a,l*]PDE) (Scheme 1). These enzymes function with high stereoselectivity in mammalian systems. Previous animal studies (mouse skin, lung, ovary and rat mammary gland) have shown that the tumorigenic activity of DB[*a,l*]P is predominantly mediated through genotoxic fjord region (−)-*anti*- and (+)-*syn*-DB[*a,l*]PDE (7;12–15). The DNA binding of DB[*a,l*]P is primarily mediated by (−)-*anti*-DB[*a,l*]PDE and to a smaller extent, by (+)-*syn*-DB[*a,l*]PDE, forming covalent DB[*a,l*]PDE-$N^6$-dA and -$N^2$-dG adducts, with adenine adducts frequently predominant (7;16). However, the metabolic activation of DB[*a,l*]P has not been examined in the mouse oral tissues. Thus, it is important to detect and quantify stereospecific DNA adducts derived from metabolically activated intermediates that can damage DNA, which can account for the genotoxic mechanism of DB[*a,l*]P-induced oral carcinogenesis in mice. In addition, literature data revealed that different stereospecific adducts possess varied biological activities (17). Compared with other detection methods, such as $^{32}$P-postlabelling and immunoassays, high-performance liquid chromatography-tandem mass spectrometry (HPLC-MS/MS) method, using synthetic internal standards, can provide more specific information about structure of the adduct (3). Here we developed a stable isotope dilution LC-MS/MS method for the detection and quantification of *anti*-DB[*a,l*]PDE-$N^6$-dA adduct isomers *in vivo*. The internal standards [$^{15}N_5$]-(±)-*anti*-DB[*a,l*]PDE-$N^6$-dA adducts were synthesized and the stereochemistry of each isomer was characterized by mass spectrometry (MS), nuclear magnetic resonance (NMR) and circular dichroism (CD) analysis, according to published procedures. In addition, to understand the biological fate of these adducts, we studied the formation and disappearance of adducts as a function of time, in the oral tissues of mice treated with DB[*a,l*]P. The results demonstrate that DB[*a,l*]P is primarily metabolized to (−)-*anti*-DB[*a,l*]PDE in the oral tissues of mice, consistent with studies in other preclinical model systems (7;15;18;19).

## MATERIALS AND METHODS

### Caution

*DB[a,l]P and DB[a,l]PDE are mutagenic and carcinogenic. They should be handled with extreme care, following NCI safety guidelines (http://pubs.acs.org/doi/abs/10.1021/ed052pA419).*

### Chemicals

DB[*a,l*]P and (±)-*anti*-DB[*a,l*]PDE were prepared according to a published method by our group (20). [$^{15}N_5$]-dA was obtained from Spectra Stable Isotopes (Columbia, MD). Solvents, other chemicals and enzymes used in the present study were obtained from Sigma-Aldrich (St. Louis, MO).

### Synthesis and structural characterization of adduct standards

(±)-*anti*-DB[*a,l*]PDE-$N^6$-dA adducts were prepared according to a method published previously (21). They were synthesized by a direct reaction of racemic (±)-*anti*-DB[*a,l*]PDE [2 mg, dissolved in 400 μL dry dimethylformamide (DMF) under $N_2$] with excess dA (15.3 mg) at 100 °C for 30 min. DMF was then removed under vacuum; the residue was dissolved in DMSO/$CH_3OH$ (1:1). The adducts were purified on a reversed-phase YMC ODS-AQ 5 μm, 120 Å column (6.0 mm × 250 mm) (YMC, Wilmington, NC), using a $CH_3CN/H_2O$ gradient, following the methods reported by Li *et al* (21). Each eluted fraction was further purified by 70% isocratic $CH_3OH/H_2O$ using the same column (21). Both of the purifications were carried out on an Agilent series 1100 HPLC system (Agilent Technologies, Palo Alto, CA). The structure and stereochemistry of adducts were confirmed by a combination of UV, MS, $^1H$ NMR and CD spectral analysis. The concentration of each purified stereoisomer was determined by UV spectroscopy (Beckman Coulter DU 640 spectrophotometer), ($\varepsilon$=43000 $M^{-1}cm^{-1}$) (22). The MS/MS analysis was conducted by an API 3200™ LC/MS/MS triple quadrupole mass spectrometer (Applied Biosystem). The $^1H$ NMR spectra were recorded in DMSO-$d_6$ at 600 MHz on a Bruker Avance NMR spectrometer. The CD spectra were recorded in methanol on a Jasco J-815 CD spectrometer.

The $^{15}N$-labeled internal standard [$^{15}N_5$]-(±)-*anti*-DB[*a,l*]PDE-$N^6$-dA adducts were prepared and characterized essentially following the same approach described above for unlabeled adducts, except using [$^{15}N_5$]- deoxyadenosine.

### Animal treatment with DB[*a,l*]P and DB[*a,l*]PDE

Female B6C3F1 mice (Jackson Laboratories, Bar Harbor, ME), 6 weeks of age, were used in this study. The bioassays were carried out in accordance with NIH Guide for the Care and Use of Laboratory Animals and were approved by Institutional Animal Care and Use Committee. Initially, short-term studies were performed to determine whether our HPLC-MS/MS method is sensitive enough to detect DNA adducts *in vivo* in the oral tissues of treated mice. A group of three mice was treated with 12 nmol of DB[*a,l*]PDE topically into the oral cavity, and sacrificed at 48 h after the treatment. Another group of three mice was treated with 240 nmol DB[*a,l*]P per day for 2 days, sacrificed at 24 h after the second carcinogen dose. Finally, we carried out a time-course study and mice were treated with 24 nmol DB[*a,l*]P topically into the oral cavity 3 times per week for 5 weeks. Six animals per group were sacrificed at 48 h, 1, 2 and 4 weeks after the last dose. At termination, mice were sacrificed by $CO_2$ asphyxiation; soft tissues of the oral cavity, including buccal mucosa, floor of the mouth as well as soft tissues attached to the hard palate, were collected and pooled together for DNA adduct analysis.

### DNA extraction from animal tissues

DNA isolation was performed using the Qiagen genomic DNA isolation procedure. Homogenized oral tissues were incubated with RNase A and proteinase K for 2 h. The DNA was purified with Qiagen genomic tips (500/G). DNA was dissolved in TE buffer pH=8.0. The concentration was determined by the absorbance at 260 nm using a NanoDrop ND-1000 spectrophotometer (NanoDrop Technologies, Wilmington, DE).

### DNA hydrolysis and solid phase extraction

Prior to enzymatic digestion, 400 pg [$^{15}N_5$]-anti-DB[*a,l*]PDE-dA adduct were added to 200 μg DNA isolated from oral tissues of mice treated with DB[*a,l*]P or DB[*a,l*]PDE. To the DNA solution, 1M $MgCl_2$ (10 μL/mg DNA) and DNase I (0.2 mg/mg DNA) were added and incubated at 37 °C for 1.5 h. Nuclease P1 (20 μg/mg DNA) was added and the mixture was incubated at 37 °C for 1.5 h. Then snake venom phosphodiesterase (0.08 units/mg

DNA) and alkaline phosphatase (2 units/mg DNA) were added after adjusting the pH to 9 with 0.1 M tris buffer (pH=9.0). The mixture was incubated at 37 °C overnight (~ 18 h) (23). The digested DNA sample was centrifuged at 14000 rpm for 10 min. An aliquot of the supernatant was subjected to HPLC analysis to assess the dA level. The remaining supernatant was subjected to solid phase extraction using an Oasis HLB column (1 $cm^3$, 30 mg, Waters Ltd.). The column was initially conditioned with 1.0 mL of methanol followed by 1.0 mL of HPLC grade water. The digested DNA sample was then loaded onto the column and washed with 1.0 mL of methanol: water (5:95 v/v) (24). The DB[*a,l*]PDE-dA adducts were eluted from the column with methanol, and the eluent were concentrated under mild $N_2$ stream.

### HPLC-MS/MS analysis

The analysis was carried out on a API 3200™ LC/MS/MS triple quadrupole mass spectrometer interfaced with an Agilent 1200 series HPLC using an Agilent extend-c18 5 μm 4.6 × 150 mm column. The electrospray ionization (ESI) was performed in the positive mode. The MS parameters were set as follows: electrospray source temperature and voltage were 400°C and 5.5 kV, respectively; the declustering potential (DP), collision energy (CE), entrance potential (EP), and cell exit potential (CXP) were optimized as 56, 33, 7.5 and 8 ev respectively; the collision activated dissociation (CAD) gas was set at 5 psi, while the curtain gas was set at 20 psi. The elution solvent program was 200 μL/min gradient using solvent A (methanol containing 0.1% formic acid) and solvent B (water containing 0.1% formic acid). The gradient was 10% A to 70% A in 5 min, followed by 70% A in 10 min, continued to 90% A in 30 min, and 90% A was held for another 5 min. Adducts were monitored in multiple reaction monitoring (MRM) mode. The MS/MS transitions of *m/z* 604→ *m/z* 335, and *m/z* 609→ *m/z* 335 were monitored for targeted adducts and internal standards, respectively.

### Calibration curves for DNA-adducts

Calibration curves were constructed by mixing authentic unlabelled adduct (5, 20, 50, 200, 500 pg), 200 pg of $N^{15}$ internal standard adduct and 100 μg of DNA obtained from oral tissues of untreated mice. The mixture was subjected to the same DNA digestion and adducts purification procedure for HPLC-MS/MS analysis as described above. Statistical significance was analyzed by student's *t* test.

## RESULTS

### Stereochemical characterization of adduct standards

Using a previously published method, the four synthetic stereoisomeric adducts, formed from the incubation of (±)-*anti*-DB[*a,l*]PDE with dA were prepared (a representative HPLC UV chromatogram can be found in Figure S1 in the supporting information). The structure and stereochemistry of the adduct stereoisomers were identified and characterized by a combination of MS, NMR and CD spectra. A full scan ESI-MS of DB[*a,l*]PDE-$N^6$-dA adducts was conducted at the positive mode, indicating the presence of protonated molecule ion $[m+H]^+$ at *m/z* 604. The fragmentation patterns of the molecular ions are similar among these adducts with the presence of *m/z* 353, 335, 317, 307, with fragment 335 being the strongest signal. The MS/MS fragments of stable isotope labeled internal standards [$^{15}N_5$]-DB[*a,l*]PDE-dA [$(m+H)^+$ at *m/z* 609] were similar to unlabeled adducts (Figure S2 in the supporting information). A comparison of our $^1H$ NMR spectra (data not shown) of the four adducts (peaks 1–4) with data published by Yagi *et al* (25), revealed a marked downfield shift (0.5 ppm) for the fjord region $C_{14}$-H signal of the *cis*-adducts, compared to that of the *trans*-adducts. The CD spectra were also acquired to identify the stereochemistry of each adduct (Figure S3 in the supporting information). Each pair of enantiomeric adducts

exhibited symmetrical CD spectra, but were opposite in sign. The sign of the signal at ~270 nm was used to assign the empirical configuration (26–28). Consistent with corresponding peaks assignment reported by Yagi *et al* (25) and Ruan *et al* (29), in terms of the elution order, the four synthetic adducts are assigned as (+)-*anti*-*cis*-, (−)-*anti*-*cis*-, (−)-*anti*-*trans*-, (+)-*anti*-*trans*-DB[*a,l*]PDE-$N^6$-dA adduct, respectively (Chart 1).

### Identification of DB[*a,l*]PDE DNA adducts in oral tissues of mice

The LC-MS/MS method was used to identify DNA adducts *in vivo* following topical application of (±)-*anti*-DB[*a,l*]PDE into the oral cavity of mice. This method revealed the formation of four adducts (Figure 1A). In contrast, we detected two adducts in oral tissues of mice treated with the parent compound DB[*a,l*]P (Figure 1B). The co-elution of the internal standards and analytes, identified as (−)-*anti*-*cis* and (−)-*anti*-*trans*-DB[*a,l*]PDE-dA adducts, were observed (Figure 1C).

Calibration curves were constructed for the two (−)-*anti*-cis-DB[*a,l*]PDE-dA and (−)-*anti*-*trans*-DB[*a,l*]PDE-dA adducts, which were detected with the matrix of 100 μg digested DNA. Both calibration curves appear to be linear ($r^2 = 0.998$ and $r^2 = 0.999$, respectively illustrated in Figure 2). The detection limits for dA adducts were 8 fmol using 100 μg digested DNA obtained from oral tissue of mice as the matrix.

The time-course study of the two adducts following multiple dose of DB[*a,l*]P, revealed a time-dependent disappearance pattern at 48 h, 1, 2, and 4 weeks after the last carcinogen administration. The results are summarized in Table 1 and Figure 3; The levels of (−)-*anti*-*trans*-DB[*a,l*]PDE-dA adduct were consistently significantly higher than (−)-*anti*-*cis*-DB[*a,l*]PDE-dA adduct over the time course post-treatment ($p < 0.005$). At 4 weeks after the last dose, a significant decrease in the level of (−)-*anti*-*cis*-DB[*a,l*]PDE-dA adduct was observed compared with the level at 48 h after ($p < 0.05$). For (−)-*anti*-*trans*-adduct, compared with levels at 48 h after the last dose of carcinogen, the levels of adducts decreased significantly at other time points, 1 week ($p < 0.05$), 2 weeks ($p < 0.005$), and 4 weeks ($p < 0.005$). There is a significant difference between 1 week and 2 weeks ($p < 0.05$) and also between 1 week and 4 weeks after last dose ($p < 0.05$). However, the levels remained relatively constant at 2 and 4 weeks post treatment for (−)-*anti*-*trans*-DB[*a,l*]PDE-dA adduct. The slopes of the lines for two adducts indicated that the rate of disappearance of (−)-*anti*-*trans*-DB[*a,l*]PDE-dA adduct is faster than (−)-*anti*-*cis*-DB[*a,l*]PDE-dA adduct in mice oral tissues within the first 4 weeks after the treatment of DB[*a,l*]P (Figure 3).

## DISCUSSION

In the present study, we developed a LC-MS/MS method for the detection of *anti*-DB[*a,l*]PDE-$N^6$-dA adducts *in vivo*. We detected two adducts derived from (−)-*anti*-DB[*a,l*]PDE in oral tissues of mice treated with DB[*a,l*]P. This result suggests that under the conditions of our experimental protocol, DB[*a,l*]P can be metabolized to (−)-*anti*-DB[*a,l*]PDE. Our result is consistent with those reported previously; it has been shown that in human cells, mouse skin, mouse embryo cells, and cells expressing recombinant CYP enzymes, metabolic activation of DB[*a,l*]P result in the predominant formation of (−)-*anti*-DB[*a,l*]PDE-DNA adducts (7;30–33). Similarly, using $^{33}$P-postlabeling method, Mahadevan *et al* had shown that the majority of DNA adducts formed in the lungs of mice exposed to DB[*a,l*]P were mainly derived from (−)-*anti*-DB[*a,l*]PDE (18).

In mice, DB[*a,l*]P is known to induce CYP1A1 and CYP1B1 in several tissues (34;35). Previous studies have shown that CYP1A1 and CYP1B1 differ in their regio- and stereochemical selectivity of activation of DB[*a,l*]P, with higher proportion of (−)-*anti*-DB[*a,l*]PDE formed by CYP1B1 (8) . In addition, Buters *et al* had reported that CYP1B1-

dependent formation of the DNA-reactive (−)-*anti*-DB[*a,l*]PDE represents the critical step in DB[*a,l*]P-induced tumor formation (15). Whether CYP1B1 is much more prevalent than CYP1A1 in mouse oral tissues remains to be elucidated. Another possibility is that (+)-*syn*-DB[*a,l*]PDE may have been formed in mouse oral tissues, but the levels of dA adducts derived from it were lower than the detection limit of our LC-MS/MS method.

In the present study, we focused on the detection and quantification of *anti*-DB[*a,l*]PDE-dA adducts in the oral tissues of mice treated with DB[*a,l*]P. The rational to initially focus on detecting dA adducts but not dG adducts, was based on the intrinsic structural properties of sterically hindered fjord region dihydrodiol epxoides, which predominantly bind to dA residues in native DNA (36). In general, animal studies have shown that fjord region PAHs are much more tumorigenic than bay region PAHs; however, there are exceptions, such as benzo[*c*]phenanthrene (B[*c*]Ph). Fjord region PAHs, like DB[*a,l*]P, predominantly bind dA residues in DNA, while binding to dG residues at a lower frequency . In contrast, bay region PAHs, such as benzo[*a*]pyrene (B[*a*]P), are known to form $N^2$-dG adduct at a much higher frequency than $N^6$-dA adduct (7). This carcinogen-DNA binding specificity is mainly ascribed to intrinsic chemical properties of the PAH molecules, rather than the influence by the tissues.

Bulky PAH-DNA adducts are generally removed by nucleotide excision repair (NER) (37;38). It has been observed that dA adducts derived from several fjord PAH diol epoxides, including DB[*a,l*]PDE-$N^6$-dA adducts are resistant to NER (39;40). Studies in human cell extracts have also shown that DB[*a,l*]PDE-$N^6$-dA adducts are more resistant to NER system than DB[*a,l*]PDE-$N^2$-dG adducts, which suggest that DB[*a,l*]PDE-$N^6$-dA adducts may persist longer and may have higher mutagenic potential than DB[*a,l*]PDE-$N^2$-dG adducts (41). The structural features of fjord PAH diol epxodie- $N^6$-dA adducts render them more resistant to NER, leading to persistence of longer-lived adducts, which are expected to enhance the frequencies of mutations in mammalian cells or inhibit transcription (42;43).

Formation of DNA adducts derived primarily from dA, combined with their higher resistance to DNA repair suggest the importance of these adducts in DB[*a,l*]P induced carcinogenesis. Therefore, certain DB[*a,l*]PDE-$N^6$-dA adducts may persist longer and result in an increased mutagenic and carcinogenic potential, which can play important roles during the initiation of DB[*a,l*]P-induced oral carcinogenesis.

Regarding removal efficiency, the levels of (−)-*anti-cis*-DB[*a,l*]PDE-dA adduct were not altered significantly until 4 weeks after the last carcinogen treatment, while the levels of (−)-*anti-trans*- DB[*a,l*]PDE-dA adduct decreased significantly throughout the time course examined in the present study after the last carcinogen treatment. We observed a relatively faster rate of removal of (−)-*anti-trans*-DB[*a,l*]PDE-dA adduct within the first 2 weeks after treatment, followed by a slower rate of removal from 2 to 4 weeks after administration. The efficiencies of DNA repair depend on the stereochemical properties of adducts. Our results indicate that (−)-*anti-cis*-DB[*a,l*]PDE-dA adduct may be more resistant to NER compared to (−)-*anti-trans*-DB[*a,l*]PDE-dA adduct. Dreij *et al* has shown that when human A549 epithelial lung carcinoma cells are exposed to 0.1 μM of (−)-*anti*-DB[*a,l*]PDE up to 6 h, the levels of *trans*- adduct do not change, while there are significant increases for (−)-*anti-cis*-DB[*a,l*]PDE-dA adduct within 6 h after the treatment (44). Although the structural features of (−)-*anti-cis*-DB[*a,l*]PDE-dA adduct have not yet been defined, the adduct may adopt a stable structure in DNA duplex which is less recognizable by cellular sensor and repair system.

In the present study, detection and quantification of *anti*-DB[*a,l*]PDE-dA adducts in mouse oral cavity within one month following a 5-week DB[*a,l*]P treatment, not only explored the

genotoxic mechanism of DB[*a,l*]P induced oral carcinogenesis, but also helped to explain the mutagenesis of DB[*a,l*]P in this mouse oral cancer model (10). The formation of DNA adducts reflects chemical-specific genetic damage, which is prerequisite for the initiation of carcinogenesis. These results suggest the critical role of DB[*a,l*]PDE in the development of DB[*a,l*]P-induced oral carcinogenesis (10). Thus, the development of a novel oral cancer model employing DB[*a,l*]PDE in the mouse oral cavity would be desirable.

In summary, Our newly developed HPLC-MS/MS method is sensitive enough to detect stereospecific DB[*a,l*]PDE-dA adducts *in vivo*. Our results suggest that in mouse oral tissues, DB[*a,l*]P is stereoselectively metabolized to (−)-*anti*-DB[*a,l*]PDE predominantly. (−)-*anti*-*trans*-DB[*a,l*]PDE-dA adduct is more prevalently formed than (−)-*anti*-*cis*-DB[*a,l*]PDE-dA adduct *in vivo*. The structural features of (−)-*anti*-*cis*-DB[*a,l*]PDE-dA adduct may render it harder to be repaired by NER. The formation of (−)-*anti*-DB[*a,l*]PDE-$N^6$-dA adducts may account for the initiation of carcinogenesis in the oral tissues of mice treated with DB[*a,l*]P.

## Supplementary Material

Refer to Web version on PubMed Central for supplementary material.

## List of abbreviations

| | |
|---|---|
| **DB[*a,l*]P** | dibenzo[*a,l*]pyrene |
| **DB[*a,l*]PDE** | dibenzo[*a,l*]pyrene-11,12-dihydrodiol-13,14-epoxide |
| **PAH** | polycyclic aromatic hydrocarbon |
| **dA** | deoxyadenosine |
| **dG** | deoxyguanosine |
| **CYP** | cytochrome P450 enzymes |
| **NER** | nucleotide excision repair |

## Acknowledgments

**FUNDING SUPPORT:**

This study was supported in part by NCI Contract NO2-CB-81013-74, NCI RO1-CA100924 and by seed funds from Penn State Cancer Institute.

## Reference List

1. International Agency for Research on Cancer (IARC). Globocan 2008: cancer incidence and mortality worldwide in 2008. 2010. http://globocan.iarc.fr/.
2. Warnakulasuriya S. Global epidemiology of oral and oropharyngeal cancer. Oral Oncol. 2009; 45:309–316. [PubMed: 18804401]
3. Hecht SS. Tobacco carcinogens, their biomarkers and tobacco-induced cancer. Nat. Rev. Cancer. 2003; 3:733–744. [PubMed: 14570033]
4. Wogan GN, Hecht SS, Felton JS, Conney AH, Loeb LA. Environmental and chemical carcinogenesis. Semin. Cancer Biol. 2004; 14:473–486. [PubMed: 15489140]
5. Harvey, RG. Polycyclic aromatic hydrocarbons: chemistry and carcinogenicity. Cambridge University Press; 1991.

6. Krzeminski J, Lin JM, Amin S, Hecht SS. Synthesis of Fjord region diol epoxides as potential ultimate carcinogens of dibenzo[*a,l*]pyrene. Chem. Res. Toxicol. 1994; 7:125–129. [PubMed: 8199298]
7. Luch A. On the impact of the molecule structure in chemical carcinogenesis. EXS. 2009; 99:151–179. [PubMed: 19157061]
8. Luch A, Coffing SL, Tang YM, Schneider A, Soballa V, Greim H, Jefcoate CR, Seidel A, Greenlee WF, Baird WM, Doehmer J. Stable expression of human cytochrome P450 1B1 in V79 Chinese hamster cells and metabolically catalyzed DNA adduct formation of dibenzo[*a,l*]pyrene. Chem. Res. Toxicol. 1998; 11:686–695. [PubMed: 9625737]
9. Snook ME, Severson RF, Arrendale RF, Higman HC, Chortyk OT. Identification of high molecular-weight polynuclear aromatic-hydrocarbons in a biologically-active fraction of cigarette-smoke condensate. Beitrage Zur Tabakforschung International. 1977; 9:79–101.
10. Guttenplan J, Kosinska W, Zhao ZL, Chen KM, Aliaga C, DelTondo J, Cooper T, Sun YW, Zhang SM, Jiang K, Bruggeman R, Sharma A, Shantu A, Ahn K, El-Bayoumy K. Mutagenesis and carcinogenesis induced by dibenzo[*a,l*]pyrene in the mouse oral cavity: A potential new model for oral cancer. Int J Cancer. 2011 In press..
11. International Agency for Research on Cancer. IARC Monographs on the evaluation of carcinogenic risks to humans. Vol. 92. Lyon, France: IARC; 2010. Some non-heterocyclic polycyclic aromatic hydrocarbons and some related exposures; p. 35-818.
12. Yoon JH, Besaratinia A, Feng Z, Tang MS, Amin S, Luch A, Pfeifer GP. DNA damage, repair, and mutation induction by (+)-syn and (−)-anti-dibenzo[*a,l*]pyrene-11,12-diol-13,14-epoxides in mouse cells. Cancer Res. 2004; 64:7321–7328. [PubMed: 15492252]
13. Prahalad AK, Ross JA, Nelson GB, Roop BC, King LC, Nesnow S, Mass MJ. Dibenzo[*a,l*]pyrene-induced DNA adduction, tumorigenicity, and Ki-ras oncogene mutations in strain A/J mouse lung. Carcinogenesis. 1997; 18:1955–1963. [PubMed: 9364006]
14. Amin S, Krzeminski J, Rivenson A, Kurtzke C, Hecht SS, El-Bayoumy K. Mammary carcinogenicity in female CD rats of fjord region diol epoxides of benzo[*c*]phenanthrene, benzo[*g*]chrysene and dibenzo[*a,l*]pyrene. Carcinogenesis. 1995; 16:1971–1974. [PubMed: 7634428]
15. Buters JT, Mahadevan B, Quintanilla-Martinez L, Gonzalez FJ, Greim H, Baird WM, Luch A. Cytochrome P450 1B1 determines susceptibility to dibenzo[*a,l*]pyrene-induced tumor formation. Chem. Res. Toxicol. 2002; 15:1127–1135. [PubMed: 12230405]
16. Cai Y, Wang L, Ding S, Schwaid A, Geacintov NE, Broyde S. A bulky DNA lesion derived from a highly potent polycyclic aromatic tumorigen stabilizes nucleosome core particle structure. Biochemistry. 2010; 49:9943–9945. [PubMed: 20964331]
17. Geacintov NE, Cosman M, Hingerty BE, Amin S, Broyde S, Patel DJ. NMR solution structures of stereoisometric covalent polycyclic aromatic carcinogen-DNA adduct: principles, patterns, and diversity. Chem. Res. Toxicol. 1997; 10:111–146. [PubMed: 9049424]
18. Mahadevan B, Luch A, Bravo CF, Atkin J, Steppan LB, Pereira C, Kerkvliet NI, Baird WM. Dibenzo[*a,l*]pyrene induced DNA adduct formation in lung tissue in vivo. Cancer Lett. 2005; 227:25–32. [PubMed: 16051029]
19. Melendez-Colon VJ, Luch A, Seidel A, Baird WM. Cancer initiation by polycyclic aromatic hydrocarbons results from formation of stable DNA adducts rather than apurinic sites. Carcinogenesis. 1999; 20:1885–1891. [PubMed: 10506100]
20. Sharma AK, Kumar S, Amin S. A highly abbreviated synthesis of dibenzo[*def,p*]chrysene and its 12-methoxy derivative, a key precursor for the synthesis of the proximate and ultimate carcinogens of dibenzo[*def,p*]chrysene. J. Org. Chem. 2004; 69:3979–3982. [PubMed: 15153038]
21. Li KM, George M, Gross ML, Seidel A, Luch A, Rogan EG, Cavalieri EL. Structure elucidation of the adducts formed by fjord-region dibenzo[*a,l*]pyrene 11,12-dihydrodiol 13,14-epoxides and deoxyadenosine. Chem. Res. Toxicol. 1999; 12:758–767. [PubMed: 10490496]
22. Sundberg K, Dreij K, Seidel A, Jernstrom B. Glutathione conjugation and DNA adduct formation of dibenzo[*a,l*]pyrene and benzo[*a*]pyrene diol epoxides in V79 cells stably expressing different human glutathione transferases. Chem. Res. Toxicol. 2002; 15:170–179. [PubMed: 11849043]

23. Delclos KB, Miller DW, Lay JO Jr, Casciano DA, Walker RP, Fu PP, Kadlubar FF. Identification of C8-modified deoxyinosine and N2- and C8-modified deoxyguanosine as major products of the in vitro reaction of N-hydroxy-6-aminochrysene with DNA and the formation of these adducts in isolated rat hepatocytes treated with 6-nitrochrysene and 6-aminochrysene. Carcinogenesis. 1987; 8:1703–1709. [PubMed: 3664962]
24. Singh R, Gaskell M, Le Pla RC, Kaur B, zim-Araghi A, Roach J, Koukouves G, Souliotis VL, Kyrtopoulos SA, Farmer PB. Detection and quantitation of benzo[*a*]pyrene-derived DNA adducts in mouse liver by liquid chromatography-tandem mass spectrometry: comparison with 32P-postlabeling. Chem. Res. Toxicol. 2006; 19:868–878. [PubMed: 16780367]
25. Yagi H, Frank H, Seidel A, Jerina DM. Revised assignment of absolute configuration of the cis- and trans-N6-deoxyadenosine adducts at C14 of (+/−)-11beta,12alpha-dihydroxy-13alpha, 14alpha-epoxy-11,12,13,14-tetrahydr -odibenzo[*a*,*l*]pyrene by stereoselective synthesis. Chem. Res. Toxicol. 2008; 21:2379–2392. [PubMed: 19053320]
26. Szeliga J, Dipple A. DNA adduct formation by polycyclic aromatic hydrocarbon dihydrodiol epoxides. Chem. Res. Toxicol. 1998; 11:1–11. [PubMed: 9477220]
27. Sayer JM, Chadha A, Agarwal SK, Yeh HJC, Yagi H, Jerina DM. Covalent nucleoside adducts of benzo[*a*]pyrene 7,8-diol 9,10-epoxides - structural reinvestigation and characterization of a novel adenosine adduct on the ribose moiety. J. Org. Chem. 1991; 56:20–29.
28. Agarwal SK, Sayer JM, Yeh HJC, Pannell LK, Hilton BD, Pigott MA, Dipple A, Yagi H, Jerina DM. Chemical characterization of DNA adducts derived from the configurationally isomeric benzo[*c*]phenanthrene-3,4-diol 1,2-epoxides. J. Am. Chem. Soc. 1987; 109:2497–2504.
29. Ruan Q, Kolbanovskiy A, Zhuang P, Chen J, Krzeminski J, Amin S, Geacintov NE. Synthesis and characterization of site-specific and stereoisomeric fjord dibenzo[*a*,*l*]pyrene diol epoxide-N(6)-adenine adducts: unusual thermal stabilization of modified DNA duplexes. Chem. Res. Toxicol. 2002; 15:249–261. [PubMed: 11849052]
30. Ralston SL, Seidel A, Luch A, Platt KL, Baird WM. Stereoselective activation of dibenzo[*a*,*l*]pyrene to (−)-anti (11R,12S,13S,14R)- and (+)-syn(11S,12R,13S,14R)-11,12-diol-13,14-epoxides which bind extensively to deoxyadenosine residues of DNA in the human mammary carcinoma cell line MCF-7. Carcinogenesis. 1995; 16:2899–2907. [PubMed: 8603462]
31. Melendez-Colon VJ, Luch A, Seidel A, Baird WM. Formation of stable DNA adducts and apurinic sites upon metabolic activation of bay and fjord region polycyclic aromatic hydrocarbons in human cell cultures. Chem. Res. Toxicol. 2000; 13:10–17. [PubMed: 10649961]
32. Mahadevan B, Marston CP, Luch A, Dashwood WM, Brooks E, Pereira C, Doehmer J, Baird WM. Competitive inhibition of carcinogen-activating CYP1A1 and CYP1B1 enzymes by a standardized complex mixture of PAH extracted from coal tar. Int. J. Cancer. 2007; 120:1161–1168. [PubMed: 17187366]
33. Nesnow S, Davis C, Nelson G, Ross JA, Allison J, Adams L, King LC. Comparison of the morphological transforming activities of dibenzo[*a*,*l*]pyrene and benzo[*a*]pyrene in C3H10T1/2CL8 cells and characterization of the dibenzo[*a*,*l*]pyrene-DNA adducts. Carcinogenesis. 1997; 18:1973–1978. [PubMed: 9364008]
34. Shimada T, Fujii-Kuriyama Y. Metabolic activation of polycyclic aromatic hydrocarbons to carcinogens by cytochromes P450 1A1 and 1B1. Cancer Sci. 2004; 95:1–6. [PubMed: 14720319]
35. Courter LA, Musafia-Jeknic T, Fischer K, Bildfell R, Giovanini J, Pereira C, Baird WM. Urban dust particulate matter alters PAH-induced carcinogenesis by inhibition of CYP1A1 and CYP1B1. Toxicol. Sci. 2007; 95:63–73. [PubMed: 17060372]
36. Szeliga J, Dipple A. DNA adduct formation by polycyclic aromatic hydrocarbon dihydrodiol epoxides. Chem. Res. Toxicol. 1998; 11:1–11. [PubMed: 9477220]
37. Sancar A. DNA excision repair. Annu. Rev. Biochem. 1996; 65:43–81. [PubMed: 8811174]
38. Wood RD. DNA damage recognition during nucleotide excision repair in mammalian cells. Biochimie. 1999; 81:39–44. [PubMed: 10214908]
39. Buterin T, Hess MT, Luneva N, Geacintov NE, Amin S, Kroth H, Seidel A, Naegeli H. Unrepaired fjord region polycyclic aromatic hydrocarbon-DNA adducts in ras codon 61 mutational hot spots. Cancer Res. 2000; 60:1849–1856. [PubMed: 10766171]

40. Cai Y, Ding S, Geacintov NE, Broyde S. Intercalative Conformations of the 14R (+)- and 14S (−)-trans-anti-DB[*a,l*]P-N(6)-dA Adducts: Molecular Modeling and MD Simulations. Chem. Res. Toxicol. 2011

41. Kropachev K, Kolbanovskiy M, Rodriguez FA, Cai Y, Ding S, Zhang L, Amin S, Broyde S, Geacintov NE. Dibenzo[*a,l*]pyrene diol epoxide-adenine but not -guanine adducts are resistant to nucleotide excision repair in human cell extracts. From Abstracts of Papers, 238th ACS National Meeting, Washington, DC. Chem. Res. Toxicol. 2009; 23:282.

42. Roth RB, Amin S, Geacintov NE, Scicchitano DA. Bacteriophage T7 RNA polymerase transcription elongation is inhibited by site-specific, stereospecific benzo[*c*]phenanthrene diol epoxide DNA lesions. Biochemistry. 2001; 40:5200–5207. [PubMed: 11318642]

43. Ruan Q, Kolbanovskiy A, Zhuang P, Chen J, Krzeminski J, Amin S, Geacintov NE. Synthesis and characterization of site-specific and stereoisomeric fjord dibenzo[*a,l*]pyrene diol epoxide-N(6)-adenine adducts: unusual thermal stabilization of modified DNA duplexes. Chem. Res. Toxicol. 2002; 15:249–261. [PubMed: 11849052]

44. Dreij K, Seidel A, Jernstrom B. Differential removal of DNA adducts derived from anti-diol epoxides of dibenzo[*a,l*]pyrene and benzo[*a*]pyrene in human cells. Chem. Res. Toxicol. 2005; 18:655–664. [PubMed: 15833025]

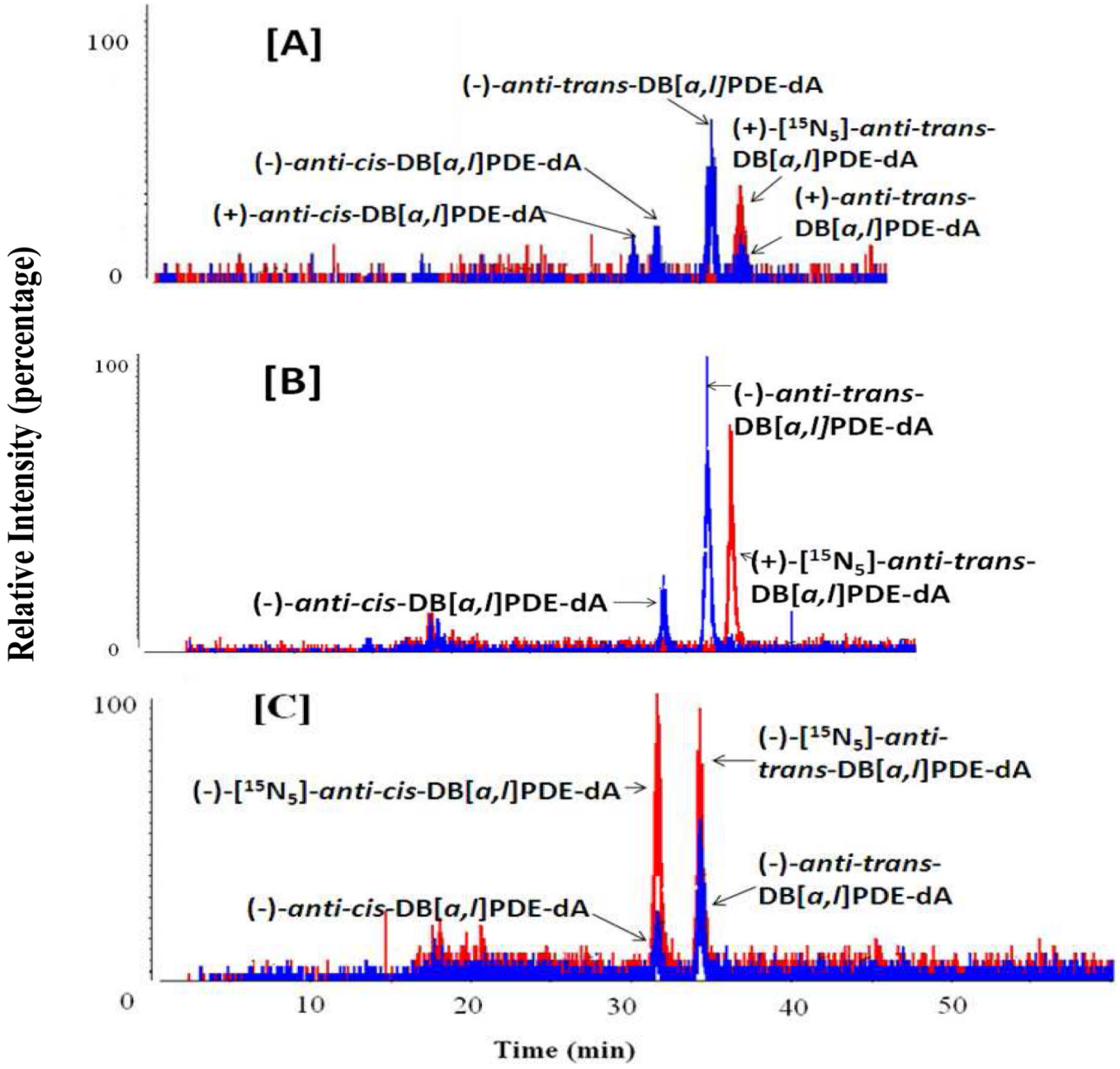


**Figure 1.**

Representative chromatograms of *anti*-DB[*a*,*l*]PDE-dA adducts obtained from stable isotope dilution HPLC-MS/MS analysis of DNA isolated from oral tissues (soft tissues of the oral cavity, including buccal mucosa, floor of the mouth as well as soft tissues attached to the hard palate were collected and pooled together for DNA adduct analysis) with (±)-DB[*a*,*l*]PDE (12 nmol and sacrificed at 48 h after) (A), of mice treated with DB[*a*,*l*]P (240 nnol per day for 2 days, sacrificed at 24 h after treatment) (B), and of mice treated with DB[*a*,*l*]P (24 nmol, 3 times per week, for 5 weeks, and sacrificed at 48 h after the last dose of carcinogen administration) (C). Peaks in red represent the added internal standard (+)-*anti*-*trans*-DB[*a*,*l*]PDE-[$^{15}N_5$]-dA adduct. Adducts detected *in vivo* are shown in blue.

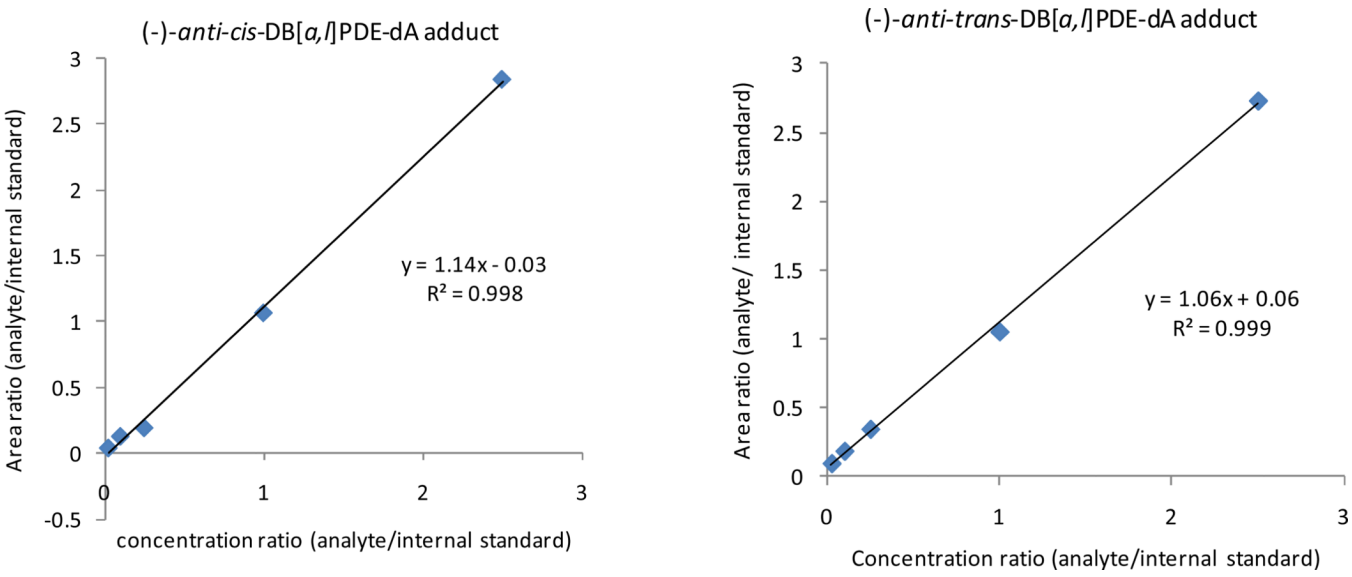


**Figure 2.**
Calibration curves for *(−)-anti-cis*- and *(−)-anti-trans* –DB[*a*,*l*]PDE-dA adducts with DNA matrix.

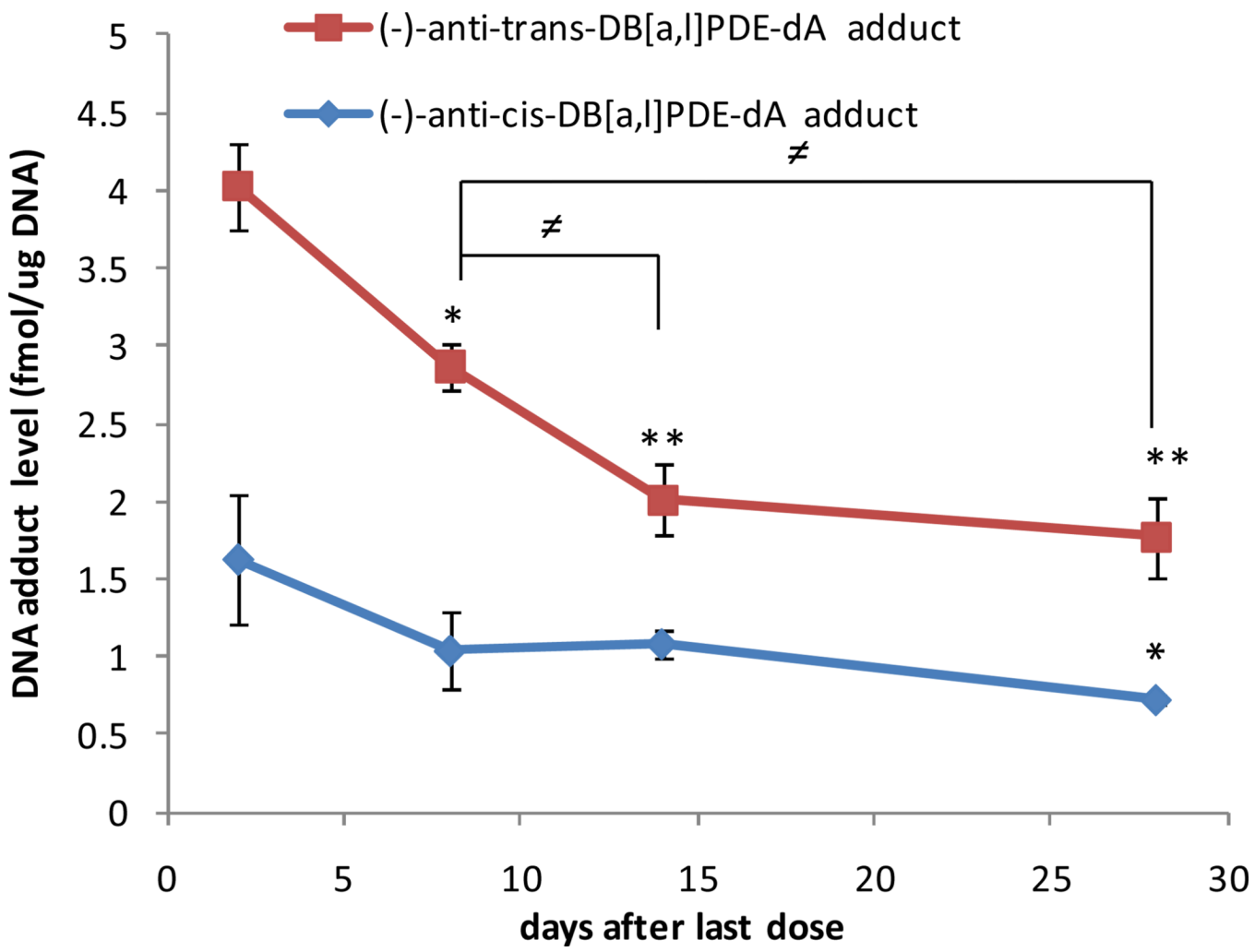


**Figure 3.**

DNA adduct levels at 2 days, 1, 2 and 4 weeks after the last dose of DB[*a*,*l*]P treatment (24 nmol, 3 times per week, for 5 weeks) in the oral tissues (same as described at Figure 1). For (−)-*anti-trans*-DB[*a*,*l*]PDE-dA adduct, a significant decrease was observed after 1 week ($^{*}$ $p < 0.05$) compared with 2 days after, and was consistently decreased after 2 and 4 weeks ($^{**}$ $p < 0.005$). In addition, levels at 2 and 4 week post treatment was also significantly lower compared to the 1 week post treatment ($^{\neq}p < 0.05$). For (−)-*anti-cis*-DB[*a*,*l*]PDE-dA adduct, DNA adduct level dropped until 4 weeks after last dose ($^{*}$ $p < 0.05$) compared with 2 days after ($n$=3).

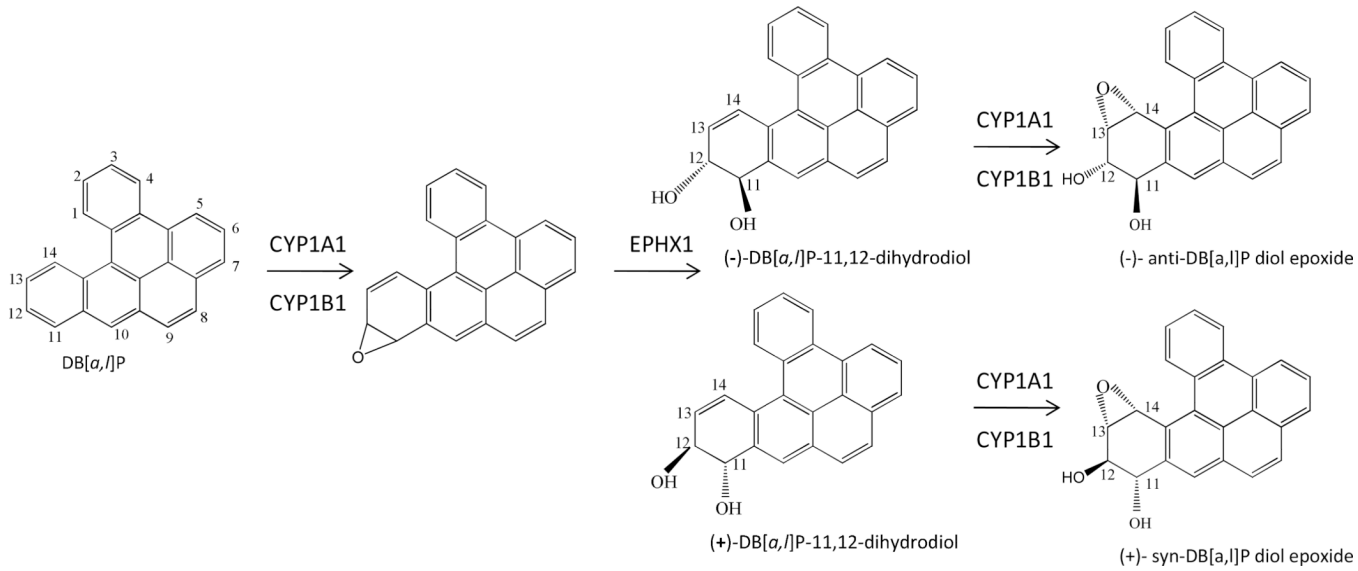


**Scheme 1.**
Metabolic activation of DB[*a*,*l*]P in mammalian systems.

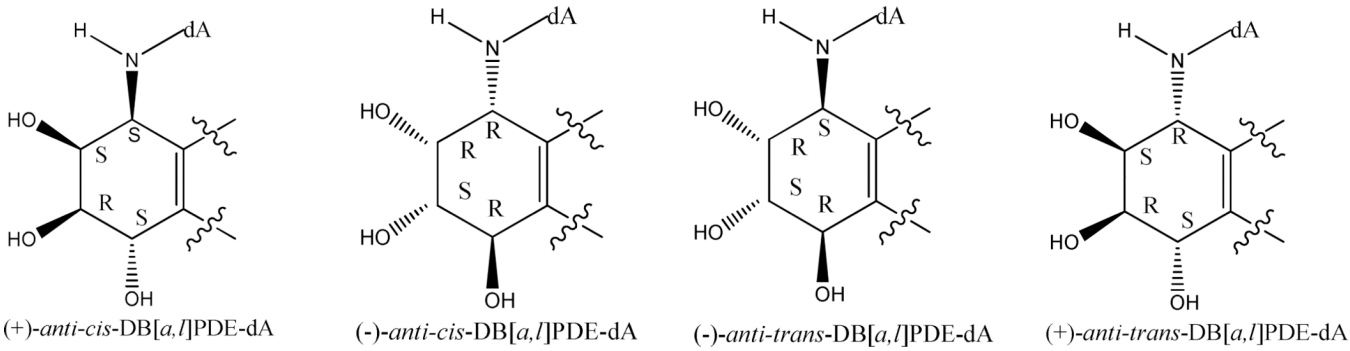


**Chart 1.**
Four synthetic standards (From left to right, in the order of elution) are depicted in abbreviated forms.

## Table 1

Analysis of DB[*a*,*l*]PDE-dA adducts from oral tissues of mice treated with DB[*a*,*l*]P

| | Average in adducts per $10^6$ deoxyadenosine [b] | |
|---|---|---|
| **days after last dose[a]** | **(−)-*anti-cis*-** | **(−)-*anti-trans*** |
| 2 | 1.6±0.4 | 3.9±0.2 |
| 7 | 1±0.2 | 2.8±0.2 |
| 14 | 1.1±0.1 | 2.2±0.3 |
| 28 | 0.8±0.04 | 1.9±0.3 |

[a] mice were sacrificed at 2 days, 1, 2 and 4 weeks after the last dose of DB[*a*,*l*]P (24 nmol, 3 times per weeks, for 5 weeks). And soft tissues of the oral cavity (including buccal mucosa, floor of the mouth and tissues attached to hard palate) were collected and pooled together for DNA adduct analysis

[b] Mean ± SD (N=3)